Geologia Série Científica USP

DOI: 10.11606/issn.2316-9095.v16i2p3-18

Revista do Instituto de Geociências - USP

Geol. USP, Sér. cient., São Paulo, v. 16, n. 2, p. 3-18, Junho 2016

SHRIMP U-Th-Pb analyses of titanites: analytical techniques and examples of terranes of the South-Southeast of Brazil – Geoscience Institute of the University of São Paulo

Análises U-Th-Pb (Shrimp) em titanitas: técnicas analíticas e exemplos em terrenos do sul-sudeste brasileiro – Instituto de Geociências da Universidade de São Paulo

Kei Sato[1], Oswaldo Siga Junior[1], Miguel Angelo Stipp Basei[1], Colombo Celso Gaeta Tassinari[1], Artur Takashi Onoe[1]

[1]Universidade de São Paulo - USP, Instituto de Geociências, Rua do Lago, 562, CEP 05508-080, São Paulo, SP, BR (keisato@usp.br; osigajr@usp.br; baseimas@usp.br; ccgtassi@usp.br; aton@usp.br)

Received on June 18th, 2015; accepted on February 12th, 2016

Abstract

Several titanite crystals were collected at Khan copper mine, Namibia, Africa. These crystals were analyzed using the Sensitive High Resolution Ion Microprobe (SHRIMP) method at the High-Resolution Geochronology Laboratory (GEOLAB), at Geoscience Institute of the University of São Paulo (IGc-USP), to be used as a reference in determining the $^{206}Pb/^{238}U$ ratios of unknown samples. In this experiment, the BLR-1 standard (1047 Ma) was used as reference, and an age of 519 Ma was obtained for the Khan internal standard. This value is very close to the ages mentioned in the literature: $^{207}Pb/^{206}Pb$ age of 518 ± 2 Ma and 522.3 ± 2.3 Ma (Thermal Ionization Mass Spectrometry – TIMS) and concordia age of 516.9 Ma (LA-ICP-MS). Analytical tests (SHRIMP dating) were conducted in titanites from two samples of granitic rocks from the Rio Piên Suite, which is considered to be a magmatic arc that bounds Curitiba and Luis Alves Terranes (South-Southeast of Brazil). The ages of 594 ± 5 Ma and 616.6 ± 2.6 Ma were obtained for samples MJ-649 and OM-629, respectively. These ages are very close to U-Pb ages measured for zircons using TIMS and SHRIMP dating. The errors for U-Pb ages in titanites are usually higher than those for U-Pb ages in zircons, which is explained by the higher concentration of common Pb in titanites. To obtain an acceptable analytical precision, more measurements are necessary. In relatively young crystals (post-Neoproterozoic Era), $^{207}Pb/^{206}Pb$ ages are very inaccurate as a consequence of the high concentration of common Pb in titanites, but, on the other hand, $^{206}Pb/^{238}U$ ages are very significant. Analyses of titanite using SHRIMP method at the GEOLAB-IGc-USP are very important, mainly when examined together with U-Pb ages for zircons and Ar-Ar ages for minerals, such as biotite and amphibole. This data allows the conduction of a precise geochronological study and the obtainment of important thermochronological data related to the uplift/denudation of rock bodies.

Keywords: Titanite; Khan; BLR; SHRIMP; Curitiba Terrane.

Resumo

Inúmeros cristais de titanita foram coletados na mina de cobre Khan, Namíbia, África. Eles foram analisados através da técnica de microssonda iônica de alta resolução e de alta sensibilidade (SHRIMP) no Laboratório de Geocronologia de Alta Resolução (GEOLab), do Instituto de Geociências da Universidade de São Paulo (IGc-USP), numa tentativa de serem utilizados como referência na determinação de razões $^{206}Pb/^{238}U$ de amostras desconhecidas. Neste experimento, foi utilizado como referência o padrão BLR1 (1.047 Ma), obtendo-se para o padrão interno Khan idade de 519 Ma. Tal valor é muito próximo das idades disponíveis na literatura especializada: idade $^{207}Pb/^{206}Pb$ de 518 ± 2 Ma e 522,3 ± 2,3 Ma (espectrômetro de massa de ionização térmica – Tims) e idade concórdia de 516,9 Ma (LA-ICP-MS). Os testes analíticos SHRIMP foram realizados em titanitas provenientes de duas amostras de rochas graníticas da Suíte Rio Piên, admitida como possível arco magmático, que baliza os terrenos Curitiba e Luis Alves (sul-sudeste brasileiro). A amostra MJ-649 acusou idade de 594 ± 5 Ma, e a amostra OM-629, idade de 616,6 ± 2,6 Ma. Tais valores são muito próximos às idades U-Pb obtidas em zircão através das técnicas SHRIMP e TIMS. Os erros obtidos nas idades U-Pb em titanitas são normalmente mais elevados que os obtidos em zircão em função da maior presença de Pb comum nas titanitas. Um maior número de medidas é aconselhável para a obtenção de uma precisão analítica aceitável. Em cristais de titanitas relativamente jovens (idades pós-neoproterozoicas), as idades $^{207}Pb/^{206}Pb$ são altamente imprecisas devido à elevada concentração de Pb comum; por outro lado, as idades $^{206}Pb/^{238}U$ apresentam valores bastante significativos. O desenvolvimento de análises em titanitas utilizando a técnica SHRIMP junto ao GEOLab-IGc-USP tem grande importância, principalmente quando acoplado a dados U-Pb obtidos em zircão e Ar-Ar em minerais, como anfibólio e biotita. Permite, além de um estudo geocronológico preciso, a obtenção de importantes parâmetros termocronológicos relacionados à ascensão/denudação de corpos rochosos.

Palavras-chave: Titanite; Khan; BLR; Shrimp; Terreno Curitiba.

INTRODUCTION

The main goal of this study is to present, in situ, new U-Pb analytical techniques, which were applied to titanites and developed with the staff of the High Resolution Geochronology Laboratory (GEOLAB) of the Geoscience Institute of University of São Paulo (USP), using the Sensitive High Resolution Ion Microprobe (SHRIMP) technique. This technique is very important for geochronological studies and for obtaining important thermochronological data, mainly when it is associated with U-Pb ages of zircon (SHRIMP and Thermal Ionization Mass Spectrometry – TIMS) and Ar-Ar/K-Ar ages of minerals. The international standards used in this study are related to titanites from samples at Khan copper mine (Namibia, Africa), with age of 519 Ma, and to BLR-1 titanites (Ontario, Canada), with age of 1047 Ma. Analyses were conducted in titanite concentrate from granitic rocks of Curitiba terrane (South-Southeast of Brazil), which was chosen because U-Pb (TIMS and SHRIMP) analyses of zircons are available for these rocks, and TIMS analysis of titanite was available for one sample (Siga Júnior, 1995; Harara, 2001; Cury, 2009).

METHODOLOGY AND ANALITICAL PROCEDURE

The titanite concentrate was obtained according to the following procedures:

- Manually breaking, crushing and grinding of samples, followed by grain size separation by sieving. The material (100-200 mesh fraction) was placed on a vibrating table (like a Wilfley table), and heavy minerals were then densimetrically separated using bromoform (d = 2.89 g/mL; 20ºC) and methylene iodide (d = 3.32 g/mL; 20ºC). The heavy material (density greater than or equal to 3.32 g/mL) was then electromagnetically separated using a Frantz separator. After magnetic minerals were removed using a hand magnet, the fraction was separated by a Frantz magnetic separator (amperage variation). Titanites are usually concentrated in the magnetic fraction and, on the other hand, zircons are concentrated in the non-magnetic fraction. In the Frantz magnetic separator, the current and inclination adjustments are respectively 0.8–1.5 A and 10º for light brown titanite, and 0.7–1.0 A and 10º for dark brown titanite;
- Titanite crystals were selected for dating by manual hand picking, using a binocular magnifying glass and transmitted light (TL). Clear and darker crystals (dark brown color) should be preferentially selected, and crystals with inclusions and fractures should not be used. Dark titanites usually have higher concentration of uranium and, consequently, of lead. Titanites, unlike zircons, are entirely dark in cathodoluminescent (CL) images. Therefore, it is not possible to observe core/rim, oscillatory zones or igneous growth in most titanites;
- Mount preparation: titanite crystals were cast with crystals of the Khan reference standard in an epoxy resin disc with a diameter of 2.54 cm. After drying, the surface was polished (P1000-2400) up to the crystal core, and then it was polished with a 3.0 to 0.25 μm diamond paste;
- SHRIMP IIe Setup – GEOLAB - IGc - USP – primary ion beam Köhler aperture = 120 μm, beam diameter = 20-30 μm, O^{-2} beam density ~ 3 - 5 ηA, and raster time = 2 minutes. Secondary ion beam source slit = 80 μm, mass resolution > 5000 (1%) with residue less than 0.020 and with no energy filter in the electrostatic analyzer (ESA). The Khan standard (U = 584 ppm) was used to calculate U, Th and Pb concentrations in unknown samples, and also to normalize the $^{206}Pb/^{238}U$ ratio (519 Ma). Integration times for acquiring data are: $CaTi_2O_4$ (10 s), ^{204}Pb (10 s), 204.1 (10 s), ^{206}Pb (20 s), ^{207}Pb (20 s), ^{208}Pb (5 s), ^{238}U (10 s), $^{248}(ThO)$ (2 s), and $^{254}(UO)$ (3 s);
- Data acquisition and processing: SHRIMP IIe uses LabView 8.5 as a communication platform between the computer and the spectrometer by means of a SHRIMP program (version 2.90), which was developed by Australian Scientific Instruments (ASI). The calibration method is based on Ln(Pb/U) vs. Ln(UO/U) (Williams, 1998), and common Pb correction uses ^{204}Pb as basis (for further information, please see Sato et al., 2014). Data reduction was performed using the software Squid 1.06 (Ludwig, 2009).

KHAN TITANITES: CHARACTERISTICS AND USE AS STANDARD FOR SHRIMP ANALYSIS AT GEOLAB-IGC-USP

General characteristics: Khan titanites

The Khan titanites were collected from pegmatitic rocks at Khan copper mine, Namibia, Africa. Titanite crystals are abundant, reaching lengths of 500 μm or more, and euhedral. Their color ranges from dark brown (high U concentration) to light brown (low U concentration), as shown in the TL image (Figure 1). In CL images, they are dark and homogeneous (Figure 2). In these crystals, U concentration is about 22–1700 ppm, with an average of 584 ppm (Heaman, 2009), and the common Pb concentration is relatively low ($^{204}Pb/^{206}Pb < 0.002$). This mineral was the first one analyzed by Kinny and McNaughton (1994), using the isotope dilution technique (Thermal Ionization Mass Spectometer – ID-TIMS), which yielded $^{207}Pb/^{206}Pb$ ages of 518 ± 2 Ma (2 σ). Posteriorly, Heaman (2009) obtained a $^{207}Pb/^{206}Pb$ (TIMS) age of 522.2 ± 2.2 Ma, and $^{206}Pb/^{238}U$ ages ranging from 432 to 569 Ma, which indicates the presence of titanite crystals (some fragments) with discordant ages. Simonetti et al. (2006) performed U-Th-Pb measurements using Laser Ablation – Ion Coupled Plasma – Mass Spectrometer (LA-ICP-MS) and obtained a concordia age of 516 ± 4.4 Ma.

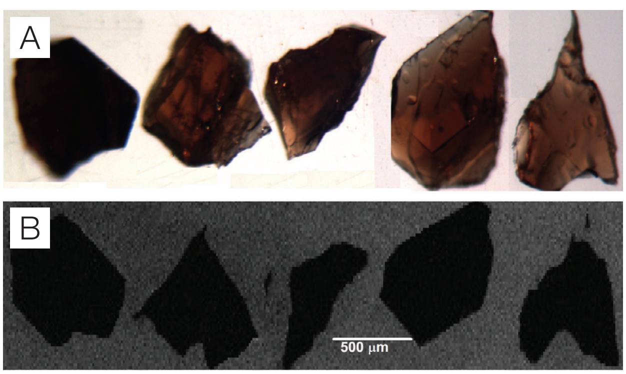

Figure 1. Khan titanite standard. (A) TL image, uranium concentration increases from right to left (light to dark brown); (B) CL image, dark color and homogeneous aspect.

Analyses were conducted in the Khan titanite using the BLR-1 titanite (Figure 2) as standard. This standard is represented by fragments of a metamorphic titanite megacrystal from Ontario, Canada. This standard is widely used for titanite dating, by Secondary Ion Mass Spectrometer (SIMS). Aleinikoff et al. (2007), using the ID-TIMS method, obtained for the BLR-1 titanite ages of 1048.0 ± 0.7 Ma ($^{207}Pb/^{235}U$, 2 σ, n = 5, mean square weighted deviation – MSWD = 2.8), 1049.9 ± 1.3 Ma ($^{207}Pb/^{206}Pb$, 2 σ, n = 5, MSWD = 2.9), and a relatively uniform age of 1047.1 ± 0.4 Ma ($^{206}Pb/^{238}U$, 2 σ, n = 5, MSWD = 0.56).

Discussion and results

SHRIMP analyses were performed in the Khan titanite using as standard the BLR-1 titanite, i. e., the Khan titanite was used as sample and the BLR-1 titanite was used to normalize the $^{206}Pb/^{238}U$ ratio. In the Khan titanite, the common ^{206}Pb concentration ranges from 0.5 to 3.8%. Total radiogenic Pb ranges from 35 to 62 ppm, with an average value of 51 ± 9 ppm. U concentration varies between 504 and 819 ppm, with an average value of 689 ± 145, and Th/U ratios vary between 0.97 and 2.3 (average of 1.3 ± 0.4, Appendix 1). U concentrations are within a similar range to the one obtained by Heaman (2009), between 229 and 1700 ppm, with an average of 584 ± 95 ppm (after outliers are removed).

It was observed that $^{207}Pb/^{206}Pb \times ^{206}Pb/^{238}U$ data (without common Pb correction) is aligned along a straight line that intercepts the concordia curve at 522 ± 16 Ma (lower intercept, Tera-Wasserburg diagram, Figure 3A). The $^{207}Pb/^{235}U$ vs. $^{206}Pb/^{238}U$ concordia diagram, with common Pb correction, is shown in Figure 3B, and yielded an age of 519.0 ± 5.1 Ma. Common Pb quantification is shown using the color scale (on the right of diagrams A and B), indicating

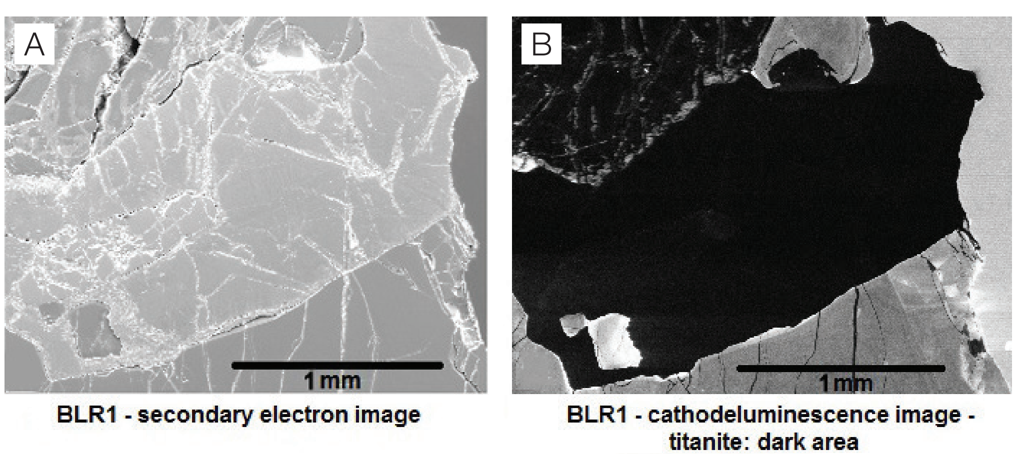

Figure 2. Titanite standard BLR-1. (A) obtained using secondary electrons; (B) obtained using CL, in which the homogeneous and dark area represents the titanite fragment.

that the higher the concentration of non-radiogenic Pb in titanites is, the greater the separation of the curve also is (Figure 3A). An increase in analytical errors was observed and, as a consequence, data uncertainty increased (increase in the ellipse major axis, Figure 3B). Figure 3C is the same as Figure 3B, but ellipses are not filled. In Figures 3D and 3E, data is shown in histograms ($^{206}Pb/^{238}U$ ages) and bar diagrams ($^{207}Pb/^{206}Pb$ ages). A unimodal Gaussian distribution, with a SHRIMP age very close to the values mentioned in the literature, was observed. It is important to highlight that Heaman (2009) obtained some discordant ages (TIMS) for the Khan titanite and, for that reason, crystals should be very carefully selected (darker crystals, without inclusions and no fractures).

GRANITIC ROCKS FROM SOUTH-SOUTHEAST OF BRAZIL SELECTED FOR SHRIMP ANALYSES OF ZIRCON AND TITANITE

Two samples of granitic rocks collected from Curitiba and Paranaguá terranes (Southern Ribeira Belt) were selected for U-Th-Pb analyses of titanites, using the SHRIMP technique (MJ-649 and OM-629). These rocks were previously analyzed using U-Pb dating in zircons and titanite (OM-629), by TIMS method. Previous results of different methods in zircons and titanites are important for introducing the methodology, allowing better evaluation of the data. For that reason, zircons of these samples were also analyzed by SHRIMP.

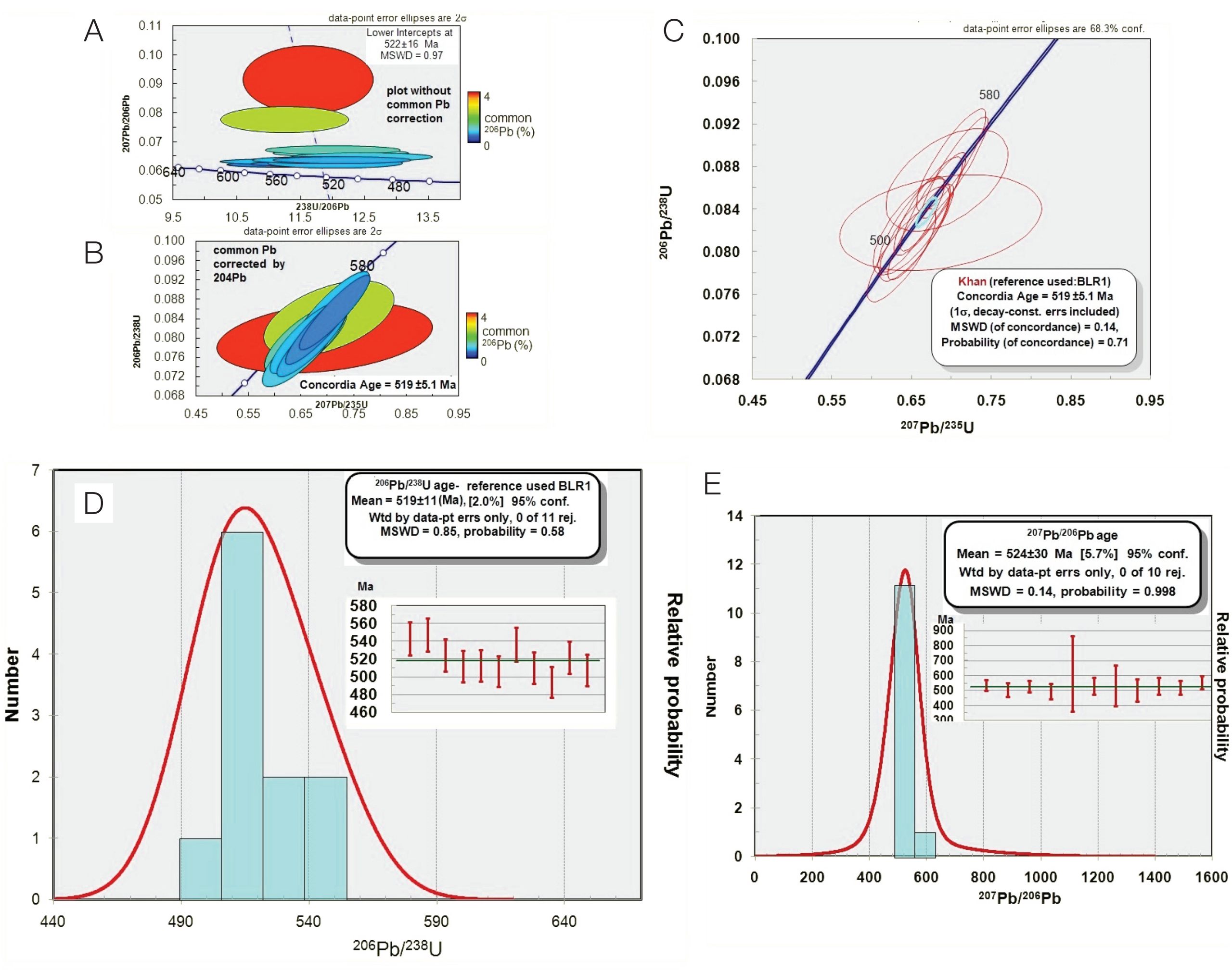

Figure 3. Standard obtained for the Khan titanite. (A) U-Pb data, Tera-Wasserburg diagram without common Pb correction; (B) concordia diagram, common Pb corrected using measured ^{204}Pb. Common Pb content (^{206}Pb %, color scale, on the right of the diagram): directly proportional to the age error; (C) data is shown in the concordia diagram (ellipses are not filled); (D) bar diagram and histogram: $^{206}Pb/^{238}U$ age (Ma); E: bar diagram and histogram: $^{207}Pb/^{206}Pb$ age (Ma). The histograms show a unimodal normal (Gaussian) distribution.

Tectonic context of the studied rocks: South-Southeast of Brazil

Geologic and geochronological studies conducted in South-Southeast of Brazil (Siga Júnior, 1995; Siga Júnior et al., 1995; 1996; 2011; Basei et al., 1998, 2011; Cury, 2009; Cury et al., 2008; Heilbron et al., 2008; Harara et al. 2001, 2002; Faleiros et al., 2011) identified four important terranes with distinctive and particular characteristics, bounded by expressive shear zones (Figure 4). Luis Alves Terrane is mainly represented by gneissic-granulitic rocks of the Paleoproterozoic (2200–2000 Ma), with some rocks inherited from the Archean (3100–2600 Ma) and some minerals of Paleoproterozoic age (2000–1800 Ma, K-Ar dating). During the Neoproterozoic, this terrane behaved as a microplate. It is limited to the north by mainly gneissic-migmatitic rocks of Curitiba Terrane (Figure 4) from Paleoproterozoic age (2200–2000 Ma) with some rocks inherited from the Archean (3100–2600 Ma), and it was extensively deformed and migmatized during the Neoproterozoic (620–600 Ma) (Siga Júnior et al., 2011). In the southern portion of Curitiba Terrane, there are deformed calc-alkaline granitic rocks (Rio Piên granitic suite) (Harara et al., 2001; 2002), which is considered be a Neoproterozoic magmatic arc. The granitic rocks selected in this study for SHRIMP U-Pb analyses of titanites are from the Rio Piên granitic suite (Figure 4). Luis Alves and Curitiba Terranes are bounded on their eastern side by an igneous belt (Paranaguá Terrane), which includes mainly granitic rocks of the Neoproterozoic (600–580 Ma) (Cury, 2009), and its host rocks are low-, medium, and high-grade metamorphic sequences. Apiaí Terrane, on the other hand (Figure 4), includes metavolcano-sedimentary sequences, mainly of the Mesoproterozoic (1500–1400 Ma), older basement cores, mainly of the Statherian (1750–1700 Ma), and secondarily sequences of the Neoproterozoic. It is located to the north of Curitiba Terrane, bounded by Lancinha shear zone (Figure 4).

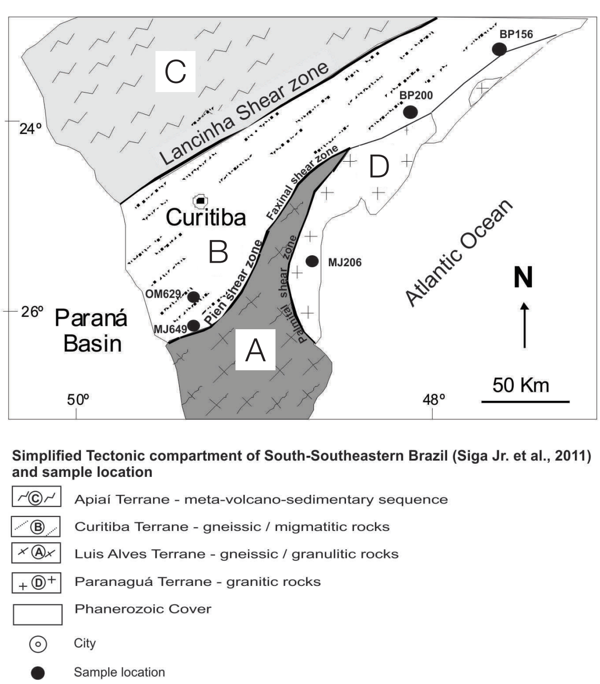

Figure 4. Simplified geological map.

Previous TIMS U-Pb Data (MJ-649 and OM-629)

Samples MJ-649 and OM-629 are deformed granitic rocks of calc-alkaline nature which occur along the northern portion of Curitiba Terrane, bounding Luis Alves Terrane (Figure 4). This granitic belt (Rio Piên granitic suite) is very important in the tectonic scenario of South-Southeast of Brazil and is considered by some authors (Basei et al., 1998, 2011; Harara et al., 2001, 2002) to be a possible Neoproterozoic magmatic arc. In previous geochronological studies, a TIMS U-Pb age of 615 ± 29 Ma (MJ-649) (Siga Júnior, 1995) was obtained for zircons, and a TIMS U-Pb age of 605 ± 5 Ma (OM-629) (Harara, 2001; Harara et al., 2002) was obtained for zircon and titanite (plotted together in the concordia diagram).

SHRIMP ANALYSES OF ZIRCONS FROM GRANITIC ROCKS OF THE SOUTH-SOUTHEAST OF BRAZIL (MJ-649 AND OM-629)

SHRIMP U-Pb analyses of zircons: MJ-649 sample

Zircon crystal, as well as some of the analyzed points (spots) of sample MJ-649 (CL image), are represented in Figure 5A. In this figure, a zircon crystal trapped inside a titanite crystal is highlighted (in Figure 5B, details are shown in TL and CL images). Since the zircon length is 40 µm, it was possible to carry out “in situU-Th-Pb isotopic analyses, using SHRIMP method. The ages are shown in a histogram (Figure 6A), bar diagram (Figure 6B), and concordia diagram (Figure 6C). The $^{206}Pb/^{238}U$ ages are represented in the first two diagrams, with a weighted average of 607 ± 5 Ma. A unimodal Gaussian distribution is observed in the histogram, indicating that only one geological event was responsible for the zircon crystallization and consequent formation of this granitic rock. In the concordia diagram ($^{206}Pb/^{238}U$ vs. $^{207}Pb/^{238}U$ ratios) (Figure 6C), the age obtained was 606.6 ± 2.6 Ma, which is very close to the $^{206}Pb/^{238}U$ average age. The TIMS U-Pb age previously determined for multiple grains was greater than that (615 Ma) (Siga Júnior, 1995), although with a relatively high error (29 Ma). It is important to point out that the zircons included in titanites (spots 1.1 and 2.1) are concordant to the others (Figure 6).

SHRIMP U-Pb analyses of zircons: OM-629 sample

Figure 7 shows zircon crystals (CL image) and analyzed points (spots) of sample OM-629. Some crystals have cores and rims, and when analyzed using SHRIMP method, they yielded Paleoproterozoic (upper intercept = 2192 ± 14 Ma) and Neoproterozoic ages (lower intercept = 613.6 ± 4 Ma) (Figure 8A). Data on the Neoproterozoic shows a bimodal distribution (histogram: Figure 8B, and bar diagram: Figure 8C), indicating that there were two different geological events in

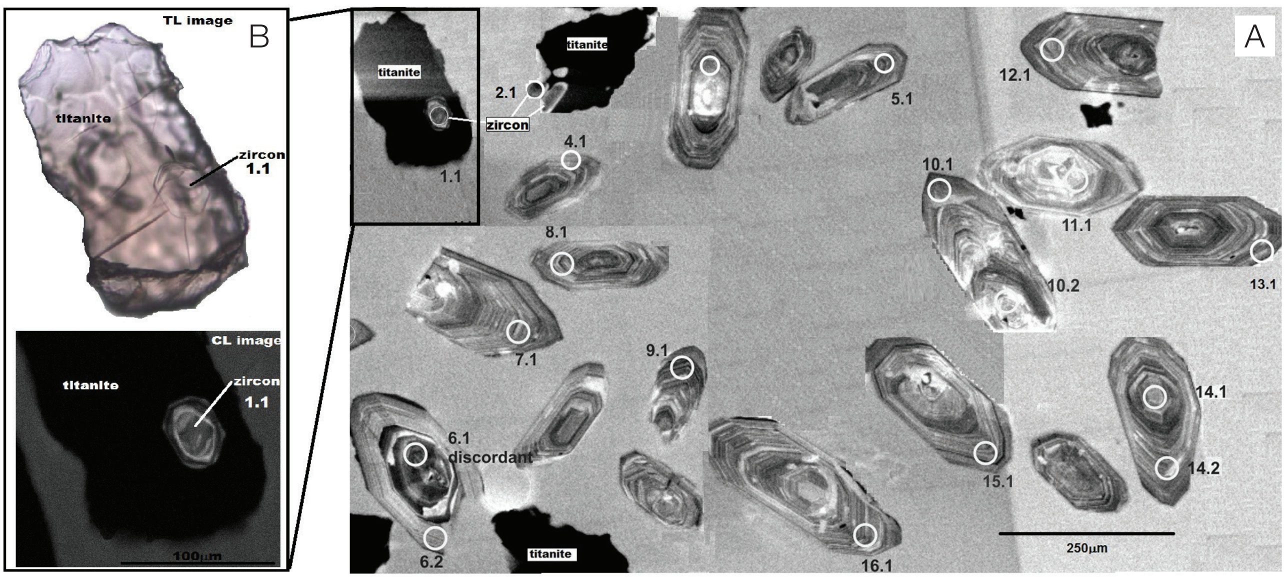

Figure 5. Sample MJ-649. (A) CL image showing the location of the analyzed points; (B) details of the zircon included in the titanite (TL image above, and CL image below).

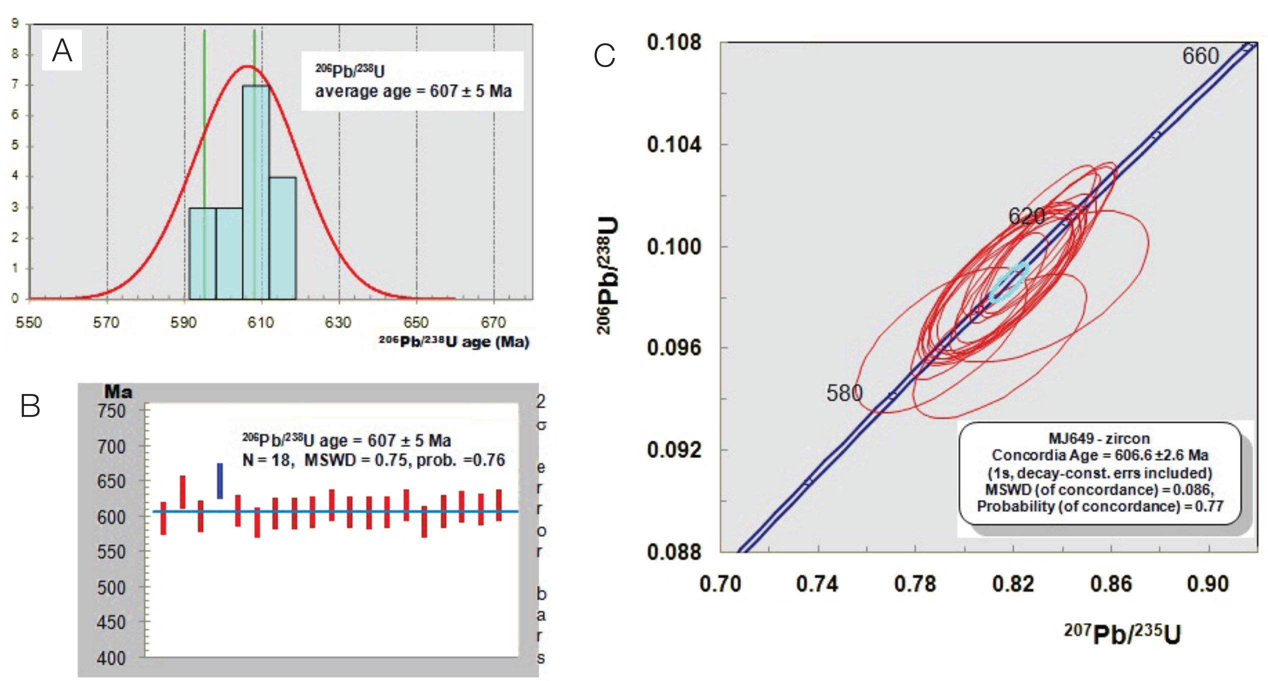

Figure 6. MJ-649 sample. (A) histogram: age vs. $^{206}Pb/^{238}U$ (Ma), unimodal normal (Gaussian) distribution; (B) bar diagram: age vs. $^{206}Pb/^{238}U$, weighted average age of 607 ± 5 Ma; (C) concordia diagram: age of 606.6 ± 2.6 Ma.

this period, with ages of 623.5 ± 4.5 Ma (F = 0.57 or 57%) and 609.0 ± 4.9 Ma (F = 0.43 or 43%), respectively. If we analyze the Neoproterozoic data all together, the average age is 615.9 ± 4.1 Ma ($^{206}Pb/^{238}U$ age) (Figure 8C) and 616.8 ± 3.4 Ma (concordia diagram: $^{207}Pb/^{235}U$ vs. $^{206}Pb/^{238}U$) (Figure 8D). In this diagram (Figure 8D), it can be clearly observed that there are two sets of values with ages of 624.7 ± 2.2 Ma and 609.2 ± 1.8 Ma, respectively. The analytical points with ages close to 625 Ma mostly correspond to zircon cores, whereas ages close to 609 Ma correspond to rims. This pattern is clearly observed in Figure 7, in which zircon 20 (spot-20) yielded an age of 625 Ma for its core (20.1) and 609 Ma for its rim (20.2). TIMS analyses of multiple zircon crystals from the same sample (OM-629) are discordant in the concordia diagram, but when those crystals are examined together with the results of TIMS analysis of titanite (concordant point), an age of 605 ± 5 Ma is obtained (Harara, 2001).

SHRIMP ANALYSES OF TITANITES FROM GRANITIC ROCKS OF SOUTH-SOUTHEAST OF BRAZIL (MJ-649 AND OM-629): USE OF THE KHAN STANDARD

Analyses of titanites from granitic rock MJ-649

Titanite crystals from sample MJ-649, including analyzed points (spots), are shown in Figure 9 (A: TL image; B: CL image). In the TL image, titanite crystals with color ranging from light to dark brown are observed, indicating a progressive increase in U concentration. In the CL image, titanite crystals appear very dark and, therefore, it was not possible to select any crystal for SHRIMP analysis.

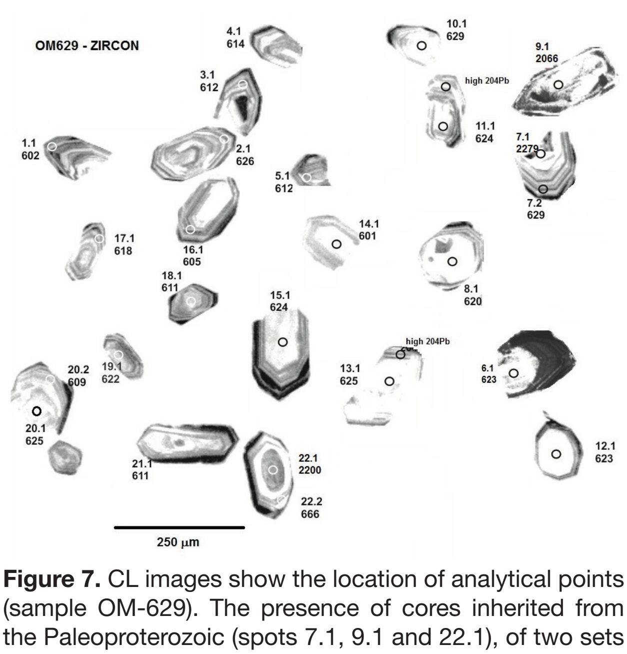

Figure 7. CL images show the location of analytical points (sample OM-629). The presence of cores inherited from the Paleoproterozoic (spots 7.1, 9.1 and 22.1), of two sets of Neoproterozoic age cores with $^{206}Pb/^{238}U$ ages ranging from 622 to 629 Ma (spots 6.1, 8.1, 10.1, 11.1, 12.1, 13.1, 15.1, 19.1 and 20.1), and of most rims with $^{206}Pb/^{238}U$ ages ranging from 602 to 612 Ma (spots 1.1, 3.1, 4.1, 5.1, 16.1, 20.2 and 21.1) can be observed.

The average concentrations of U, Th and radiogenic Pb in titanites from sample MJ-649 are 146 ± 117 ppm, 240 ± 176 ppm, and 13 ± 10 ppm, respectively (Appendix 1). Th/U ratio is approximately 2 ± 1, and common lead, 6 ± 2 % (common ^{206}Pb).

Figure 10 shows SHRIMP U-Pb data obtained for titanites from sample MJ-649 plotted on a histogram, concordia and Tera-Wasserburg diagrams. In the histogram (Figure 10A), a unimodal normal (Gaussian) distribution is shown for $^{206}Pb/^{238}U$ ages, with an average age of 594 ± 14 Ma (common Pb corrected). The high concentration of common Pb is directly related to the age error (± 14 Ma). In the concordia diagram (Figures 10B and 10D), U-Pb data indicates an age of 594.0 ± 7.1 Ma. In Figure 10C, U-Pb data (without common Pb correction) is represented in the Tera-Wasserburg diagram. It was observed that $^{207}Pb/^{206}Pb$, $^{238}U/^{206}Pb$ data are aligned along a straight line that intercepts the concordia curve at 583 ± 38 Ma. This figure shows the direct correlation between common Pb concentration (color scale, on the right of the diagram) and age precision (proximity to the lower intercept), where the concentration of common Pb is theoretically close to zero. When considering experimental errors, the ages obtained with or without common Pb correction, 594 ± 14 and 583 ± 38 Ma, respectively, are concordant.

Analyses of titanites from granitic rock OM-629

Titanite crystals from sample OM-629, including analyzed points (spots), are represented in TL image in Figure 11. The average concentrations of U, Th and Pb (radiogenic) are 78 ± 91 ppm, 208 ± 87 ppm, and 23 ± 27 ppm, respectively (Appendix 1). Th/U ratio is about 5 ± 2 (higher concentration of thorium). The concentration of common Pb (^{206}Pb) in these titanites is about 8 ± 3%, which is relatively high when compared to the Khan titanite standard (0.5 to 3.8%). More than 30 SHRIMP analyses were carried out to determine the exact age of this rock, which is affected by the low concentration of U and high concentration of common Pb in titanite crystals.

SHRIMP U-Pb data obtained for titanites from sample OM-629 ($^{206}Pb/^{238}U$ ages) is represented in the histogram (Figure 12A) and bar diagram (Figure 12B). The histogram (Figure 12A) shows a unimodal normal (Gaussian) distribution, with an age of 616.7 ± 5.0 Ma (average value). It is important to highlight that a bimodal distribution with ages of 623 ± 4.5 Ma and 609 ± 4.9 Ma was obtained for zircon crystals (SHRIMP) from this sample (Figure 8). Figures 12C

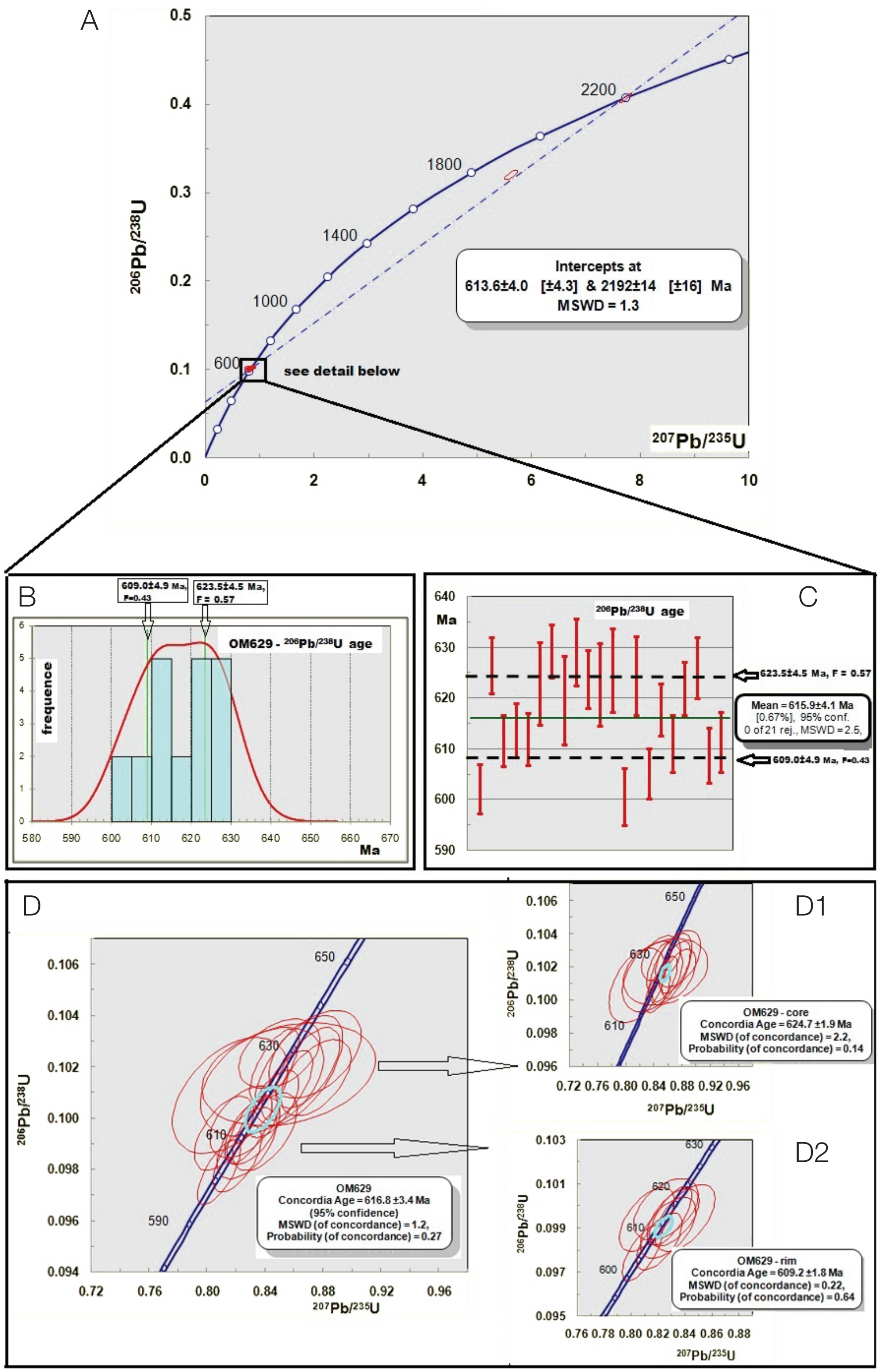

Figure 8. Graphical representation of SHRIMP U-Pb data obtained from zircons of OM-629 sample. (A) concordia diagram integrating all analytical data; (B) histogram: age vs. ^{206}Pb/^{238}U with bimodal distribution (623.5 ± 4.5 Ma, F = 0.53 or 57%, and 609.0 ± 4.9 Ma, F = 0.43 or 43%); (C) bar diagram indicating two different Neoproterozoic patterns; (D) concordia diagram: Neoproterozoic zircons with average age (core and rim) of 616.8 ± 3.4 Ma; (D1) core; (D2) rim, with ages of 624.7 ± 1.9 Ma and 609.2 ± 1.8 Ma, respectively.

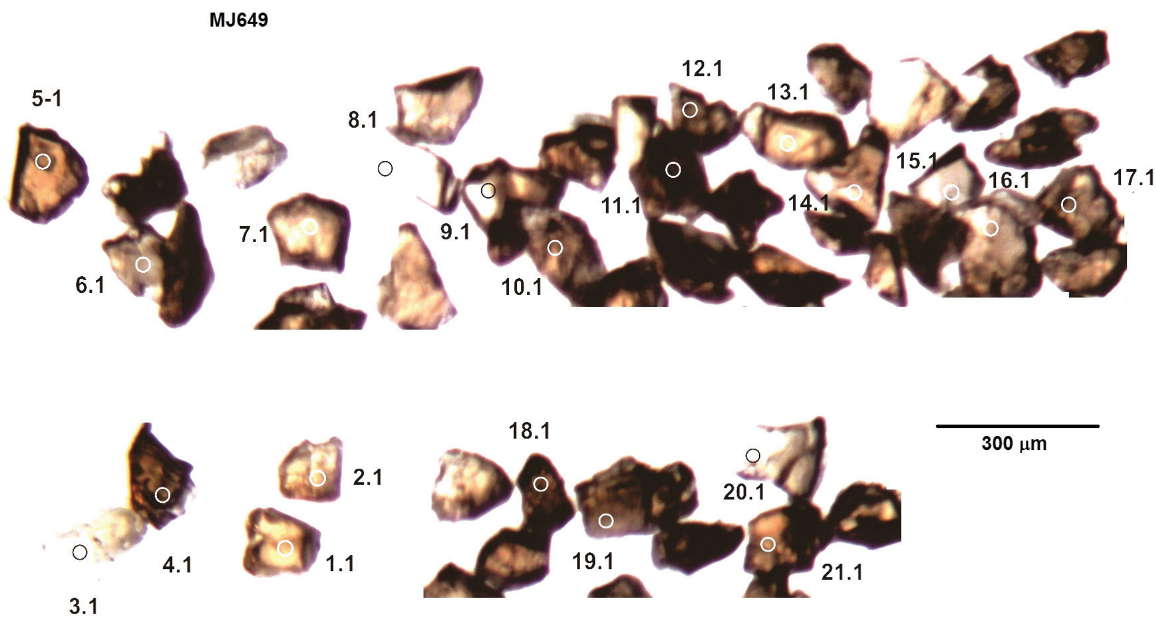

Figure 9A. TL images with the position of the analysis (spots) of titanites from MJ-649 sample (shades of brown, ranging from light to dark, indicating a progressive increase in U concentration).

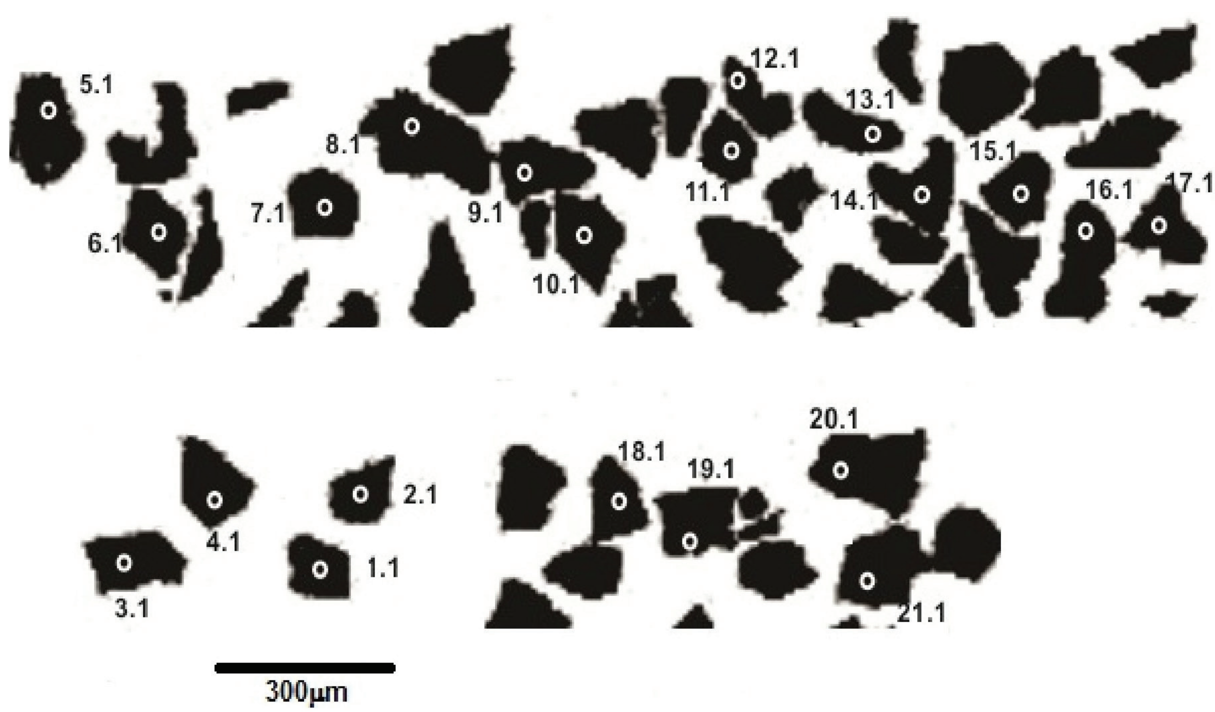

Figure 9B. CL images with the position of the analysis (spots) of titanites from MJ-649 sample. Titanite crystals are completely dark, and, therefore, it was impossible to select crystals for SHRIMP analysis.

and 12E show U-Pb data (with common Pb correction) plotted in a concordia diagram. The age of 616.6 ± 2.6 Ma was obtained in this diagram, which is very close to $^{206}Pb/^{238}U$ age (616.7 ± 5.0 Ma). In Figure 12D, U-Pb data (without common Pb correction) is shown in the Tera-Wasserburg diagram. It is observed that $^{207}Pb/^{206}Pb$, $^{238}U/^{206}Pb$ data are aligned along a straight line that intercepts the concordia curve at 627 ± 12 Ma. The differences between the titanite

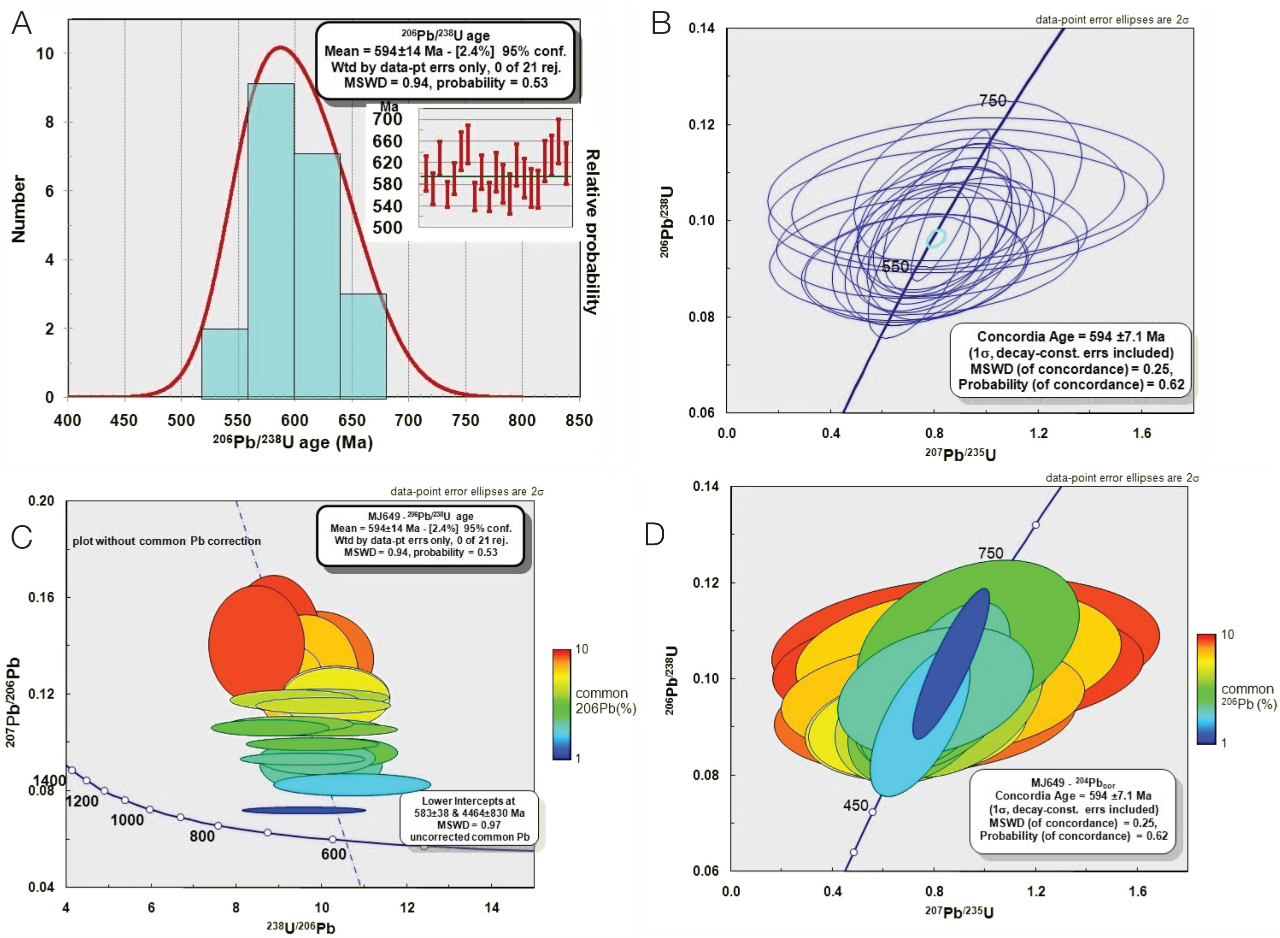

Figure 10. MJ-649 sample. (A) histogram showing a unimodal normal distribution for $^{206}Pb/^{238}U$ ages (bar diagram on the top right corner); (B) concordia diagram: age of 594 ± 7.1 (common Pb corrected using measured ^{204}Pb); (C) Tera-Wasserburg diagram (without common Pb correction); (D) the same as diagram B, but including the common ^{206}Pb representation (color scale to the right of the diagram).

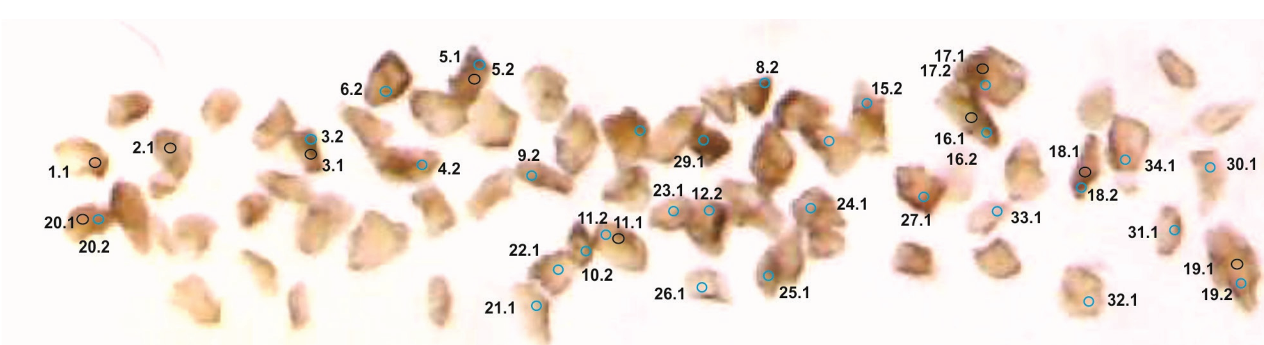

Figure 11. TL images with the position of analysis (spots) of titanites from OM-629 sample.

ages obtained by SHRIMP (616.6 Ma) and by TIMS (605 ± 5 Ma) (Harara, 2001; Harara et al., 2002) techniques may be associated in part with the Khan standard, which is not always homogeneous and concordant (Heaman, 2009).

DISCUSSION AND CONCLUSION

This article presents the first U-Pb data obtained for titanite using the SHRIMP technique at the GEOLAB-IGc-USP. Initially, Khan titanites were carefully analyzed to investigate if they could be used as a standard. In this experiment, the BLR-1 titanite standard (1047 Ma) was used as a reference (Aleinikoff et al., 2007). The BLR-1 standard had lower concentrations of common Pb and yielded more homogeneous $^{206}Pb/^{238}U$ ages and the concordant level for this standard is better than the Khan standard. The analytical data for the Khan titanite presented an average concentration of common Pb of about 2% (0.6 to 4.0% of common ^{206}Pb). SHRIMP $^{206}Pb/^{238}U$ and $^{207}Pb/^{206}Pb$ ages obtained for the selected titanite crystals (Khan) were very close (519 ± 5 Ma) with the ones mentioned in the literature (Heaman, 2009; Simonetti et al., 2006). According to Heaman (2009), some Khan titanite crystals are not completely homogeneous and are discordant, and for that reason, the crystals should be selected and analyzed carefully.

Titanites from granitic rocks of the South-Southeast of Brazil (Rio Piên granitic suite) were analyzed using the Khan titanite as a standard. The concentrations of common Pb in titanites from these granitic rocks were relatively high when compared to the ones in zircons from the same rocks. The high concentration of ^{204}Pb causes inaccuracy in the $^{207}Pb/^{206}Pb$ and $^{235}U/^{207}Pb$ ratios, mainly in younger samples (Phanerozoic). In these cases, tests showed that the number of analyses (spots) should be greater than 25. In zircons from these samples, with a relatively low concentration of common Pb, the same level of accuracy would be obtained with 12 analyses (spots). In these granitic rocks, SHRIMP U-Pb ages of titanites are very close to TIMS and SHRIMP U-Pb ages of zircon.

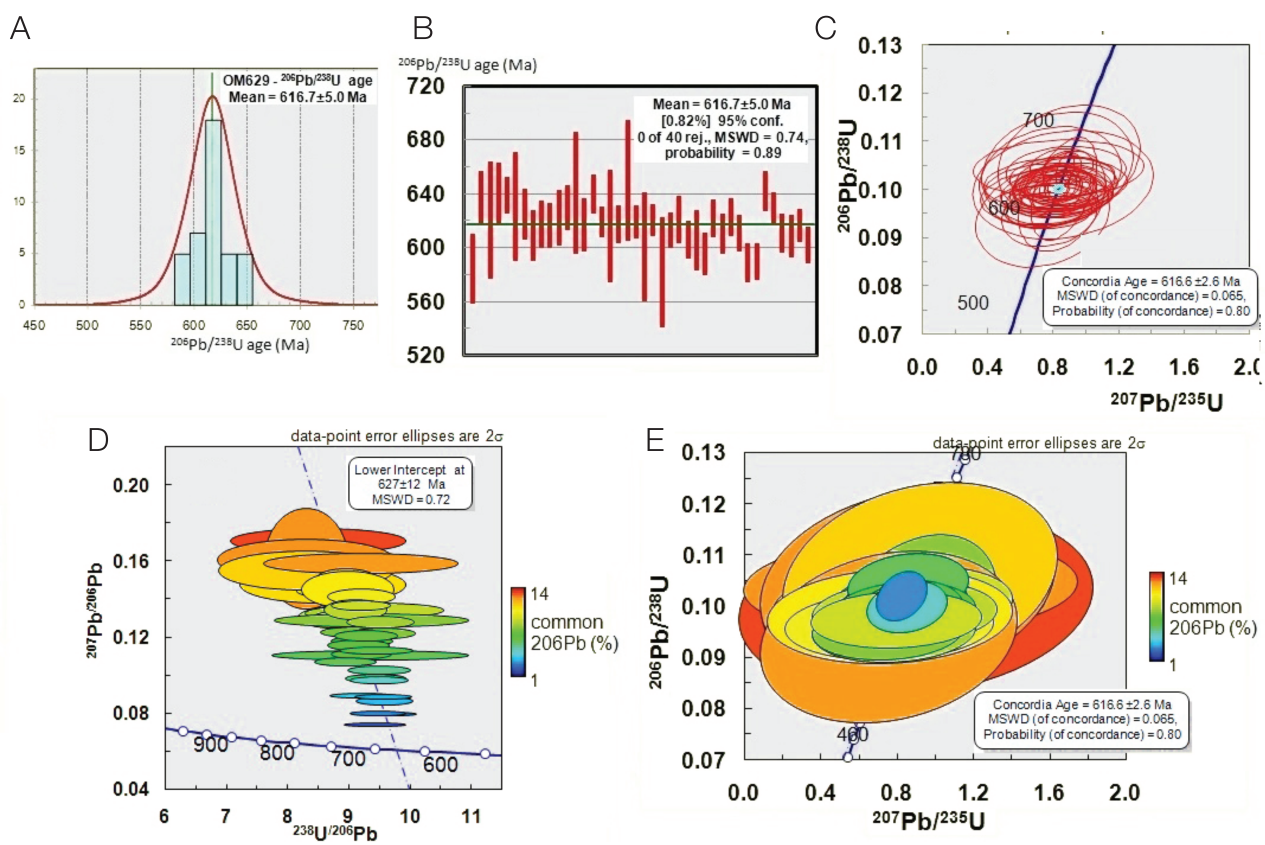

Figure 12. OM-629 sample. (A) histogram showing a unimodal normal (Gaussian) distribution ($^{206}Pb/^{238}U$ age); (B) bar diagram: weighted average of $^{206}Pb/^{238}U$ ages (616.7 ± 5.0 Ma); (C and E) concordia diagram: common Pb corrected using measured ^{204}Pb and age of 616.6 ± 2.6 Ma (MSWD = 0.065); (D) Tera-Wasserburg diagram: age of 627 ± 12 Ma (without common Pb correction). Color scale (on the right of figures D and E) represents the concentration of common Pb.

According to the specialized literature, temperatures of Pb diffusion/retention in titanites are lower than the ones observed in zircons. The values are not exact because they are affected by many factors, such as crystal size, shape and composition, as well as fluids in the environment, pressure involved in the process, and local cooling rate. In the case of titanites, these temperatures were measured by several authors, reaching up to 650ºC (Mezger, 1990; Mezger et al., 1991; Tucker et al., 1987), between 630 and 600ºC (Cherniack, 1993) and even between 800 and 710ºC (Zhang and Scharer, 1996). The granitic rocks examined in this study have a calc-alkaline nature and were possibly formed in a magmatic arc environment and, therefore, with a relatively high geothermal gradient. The ages obtained for titanite and zircon are very close, suggesting that isotherm crossing occurred relatively close in geological time. The presence of inclusions of zircon in titanites with similar ages was observed in the granitic rock MJ-649, supporting the hypothesis that these minerals were formed in a relatively short geological period of time.

ACKNOWLEDGEMENTS

The authors would like to thank the financial support from the State of São Paulo Research Foundation (FAPESP), project 2008/57861-0, and Brazilian National Council for Scientific and Technological Development (CNPq), project 573840/2008-3, National Institute of Science and Technology (INCT) of Analytical Techniques Applied to Oil and Gas Exploration; the improvements to the final version of the manuscript made through the careful reviews and suggestions by anonymous reviewers and by Leonardo Fadel Cury, from the Federal University of Paraná (UFPR). Kei Sato (project 307004/2012-0), Colombo C. G. Tassinari, Miguel A. S. Basei and Oswaldo Siga Jr. are the recipients of CNPQ research grants.

REFERENCES

Aleinikoff, J. N., Wintsch, R. P., Tollo, R. P., Unruh, D. M., Fanning, C. M., Schmitz, M. D. (2007). Ages and origins of rocks of Killingworth dome, South-Central Connecticut: implications for the tectonic evolution of Southern New England. *American Journal Science*, 307, 63-118.

Basei, M. A. S., McReath, I., Siga Júnior, O. (1998). The Santa Catarina granulite complex of Southern Brazil: a review. *Gondwana Research*, 1(3-4), 383-391.

Basei, M. A. S., Peel, E., Sánchez, E., Preciozzi, F., Nutman, A. P. (2011). The basement of Punta Del Este terrane (Uruguay): an African mesoproterozoic fragment at the eastern border of the South American Rio de La Plata craton. *International Journal of Earth Sciences,* 100(2), 289-304.

Cherniak, D. J. (1993). Lead diffusion in titanite and preliminary results on the effects of radiation damage on Pb transport. *Chemical Geology*, 110(1-3), 177-194.

Cury, F. L. (2009). *Geologia do Terreno Paranaguá*. Tese (Doutorado). São Paulo: Instituto de Geociências – USP.

Cury, L. F., Siga Júnior, O., Harara, O. M. M., Sato, K., Basei, M. A. S. (2008). Geological and geochronological setting of Paranaguá Domain, Ribeira Belt, Southern Brazil. *III International Geological Congress*. Oslo: IGC. CD-ROM.

Faleiros, F. M., Campanha, G. A. C., Martins, L., Vlach, S. R. F., Vasconcelos, P. M. (2011). Ediacaran high-pressure collision metamorphism and tectonics of the Southern Ribeira Belt (SE Brazil): evidence for terrane accretion and dispersion during Gondwana assembly. *Precambrian Research*, 189(3-4), 263-291.

Harara, O. M. M. (2001). *Mapeamento e investigação petrológica e geocronológica dos litotipos da região do Alto Rio Negro (PR-SC): um exemplo de sucessivas e distintas atividades magmáticas durante o Neoproterozóico III.* Tese (Doutorado). São Paulo: Instituto de Geociências – USP.

Harara, O. M. M., Basei, M. A. S., Siga Júnior, O. (2001). First evidence for expressive neoproterozoic intraplate mafic rocks and magma mixing in post-collisional A-PA type granites, Southern Brazil: geochemistry, U-Pb (zircon), Nd-Sr-O18 (zircon) isotope investigations. *III South American Symposium on Isotope Geology*. Pucon: UNAM. CD-ROM.

Harara, O. M. M., Basei, M. A. S., Siga Júnior, O. (2002). From subduction to late and post-collision settings: a record from neoproterozoic sucessive magmatic in the upper Rio Negro regions. *XXXXI Congresso Brasileiro de Geologia*, 1-310. João Pessoa: SBGEO.

Heaman, L. M. (2009). The application of U-Pb geochronology to mafic, ultramafic and alkaline rocks: an evolution of the three mineral standards. *Chemical Geology*, 261(1), 43-52.

Heilbron, M., Valeriano, C. M., Tassinari, C. C. G., Almeida, J. C. H., Tupinambá, M., Siga Júnior, O., Trouw, R. A. J. (2008). Correlation of neoproterozoic terranes between the Ribeira Belt, SE Brazil and its African counterpart: comparative tectonic evolution and open questions. In: R. J. Pankhurst, R. A. J. Throw, B. B. Brito Neves, M. J. Wit (Eds.), *Geological Society,* Special publication, 294, 211-238.

Kinny, P. D., McNaughton, N. J., Fanning, C. M., Maas, R. (1994). 518 Ma sphene (titanite) from Khan Pegmatite, Namibia, Southwest Africa: a potential ionmicroprobe standard. *VIII International Conference on Geochronology, Cosmochronology and Isotope Geology*, Circular 1107, 171. Denver: United States Geological Survey.

Ludwig, K. (2009). SQUID 2: a user's manual. *Berkeley Geochronology Center*, special publication, 5.

Mezger, K. (1990). Geochronology in granulites. In: D. Vielzeuf, P. Vidal (Eds.), *Granulites and crustal evolution*, 311, 451-470. Dordrecht: NATO ASI Series (Series C: Mathematical and Physical Sciences).

Mezger, K., Rawnsley, C. M., Bohlen, S. R., Hanson, G. N. (1991). U-Pb garnet, sphene, monazite, and rutile ages: implications for the duration of high-grade metamorphism and cooling histories, Adirondack Mountains, New York. *Journal of Geology*, 99, 415-428.

Sato, K., Tassinari, C. C. G. T., Basei, M. A. S., Siga Júnior, O., Onoe, A. T., de Souza, M. D. (2014). Sensitive high resolution, ion microprobe (SHRIMP IIe/MC) of the Institute of Geoscience of University of São Paulo, Brazil: analytical method and first results. *Geologia USP*, série científica, 14(3), 3-18.

Siga Júnior, O. (1995). Domínios tectônicos do sudeste do Paraná e nordeste de Santa Catarina: geocronologia e evolução crustal. Tese (Doutorado). São Paulo: Instituto de Geociências – USP.

Siga Júnior, O., Basei, M. A. S., Reis Neto, J. M., Machiavelli, A. (1996). O complexo gnáissico-migmatítico Atuba: um cinturão paleoproterozóico intensamente retrabalhado no neoproterozóico. *Congresso Brasileiro de Geologia*, Anais, 39(6), 121-123. Salvador: SBG.

Siga Júnior, O., Basei, M. A. S., Reis Neto, J. M., Machiavelli, A., Harara, O. M. (1995). O complexo Atuba: um cinturão paleoproterozóico intensamente retrabalhado no neoproterozóico. *Boletim IG-USP*, série científica, 26, 69-98.

Siga Júnior, O., Basei, M. A. S., Nutman, A., Sato, K., Passarelli, C. R., Mcreath, I., Liu, D. (2011). Extensional and colisional magmatic records in the Apiaí Terrane, South Brazil: integration of geochronological U-Pb zircon ages. *Geologia-USP*, série científica, 11(3), 149-175.

Simonetti A., Heaman L. M., Chacko T., Banerjee N. R. (2006). In situ petrographic thin section U-Pb dating of zircon, monazite, and titanite using laser ablation–MC–ICP-MS. *International Journal of Mass Spectrometry*, 253(1-2), 87-97.

Tucker, R. D., Rahiem, A., Krogh, T. E., Corfu, F. (1987). Uranium-lead zircon and titanite ages from the northern portion of western gneiss region, South-Central Norway. *Earth and Planetary Science Lett*ers, 81(2-3), 203-211.

Vlach, S. R. F., Janasi, V. A., Ulbrich, H. H. G. J. (1996). Ages and typology of the Brasiliano granitic magmatism close to the proterozoic-phanerozoic boundary, states of São Paulo and Paraná, SE-Brazil. *Anais da Academia Brasileira de Ciências*, 68, 597-598.

Watson, E. B., Wark, D. A., Thomas, J. B. (2006). Crystallization thermometers for zircon and rutile. *Contribution Mineral Petrology*, 151, 413-433.

Williams, I. S. (1998). U-Th-Pb geochronology by ion microprobe. In: M. A. McKibben, I. Shanks, W. C. P. Ridley, W. I. Ridley (Eds.), Application of microanalytical techiniques to understanding mineralizing process. *Reviews in Economic Geology*, 7, 1-35.

Zhang, L. S., Schärer, U. (1996). Inherited Pb components in magmatic titanite and their consequence of the interpretations for the U-Pb ages. *Earth and Planetary Science Letters*, 138(1-4), 57-65.

Appendix 1. SHRIMP U-Th-Pb data.

Spot Name	204 /206	% err	% comm 206	ppm U	ppm Th	$^{232}Th/^{238}U$	ppm Rad 206Pb	204 corr $^{206}Pb/^{238}U$ Age	1σ err	207 corr $^{206}Pb/^{238}U$ Age	1σ err	204 corr $^{207}Pb/^{206}Pb$ Age	1σ err	% Dis- cordant	Total 238 /206	% err	Total 207 /206	% err	238/ 206r	% err	207r /206r	% err	207r /235	% err	206r /238	% err	err correl.
Titanite																											
Khan-1.1	0.00028	16	0.50	819	930	1.17	62.1	543.1	18.7	543.4	19.0	534	35	-2	11.32	3.6	.0621	0.6	11.37	3.6	.0581	1.6	0.70	3.9	.0879	3.6	.913
Khan-2.1	0.00040	13	0.71	810	874	1.11	62.1	547.2	18.8	548.2	19.1	502	45	-8	11.20	3.6	.0631	0.6	11.28	3.6	.0573	2.0	0.70	4.1	.0886	3.6	.867
Khan-3.1	0.00030	16	0.53	740	774	1.08	54.1	524.1	18.1	524.1	18.4	529	38	1	11.74	3.6	.0623	0.6	11.80	3.6	.0580	1.7	0.68	4.0	.0847	3.6	.903
Khan-4.1	0.00039	13	0.69	723	821	1.17	51.6	511.5	17.6	511.9	17.9	493	50	-4	12.02	3.6	.0627	1.1	12.11	3.6	.0570	2.2	0.65	4.2	.0826	3.6	.847
Khan-5.1	0.00216	6	3.86	756	713	0.97	55.9	512.3	17.8	511.6	18.4	~~610~~	~~252~~	19	11.60	3.6	.0915	5.2	12.07	3.6	.0602	11.5	0.69	12.2	.0827	3.6	.295
Khan-6.1	0.00056	11	1.00	697	1019	1.51	49.4	506.2	17.5	506.0	17.7	531	58	5	12.11	3.6	.0662	0.7	12.24	3.6	.0580	2.6	0.65	4.5	.0817	3.6	.806
Khan-7.1	0.00134	7	2.40	693	722	1.08	53.0	536.2	18.8	536.9	19.2	532	137	-1	11.24	3.6	.0776	2.4	11.52	3.7	.0581	6.2	0.69	7.3	.0867	3.7	.503
Khan-8.1	0.00068	12	1.21	505	1095	2.24	36.1	510.0	17.8	510.4	18.0	501	73	-2	11.99	3.6	.0671	0.9	12.14	3.6	.0573	3.3	0.65	4.9	.0823	3.6	.736
Khan-9.1	0.00046	15	0.83	504	667	1.37	34.8	494.1	17.2	493.7	17.5	531	57	7	12.45	3.6	.0647	0.9	12.55	3.6	.0580	2.6	0.64	4.5	.0797	3.6	.812
Khan-10.1	0.00041	13	0.74	649	656	1.04	47.4	521.7	18.1	521.9	18.4	519	48	-1	11.77	3.6	.0637	0.8	11.86	3.6	.0577	2.2	0.67	4.2	.0843	3.6	.856
Khan-11.1	0.00036	14	0.64	692	732	1.09	49.0	507.2	17.6	506.6	17.9	553	43	9	12.14	3.6	.0638	0.8	12.21	3.6	.0586	2.0	0.66	4.1	.0819	3.6	.877
Mean			1.19	690	818	1.26	50.51																				
StD			1.03	105	145	0.36	8.87																				
Zircon																											
MJ-649-1.1	0.00295	10	5.24	221	157	0.73	19.5	597.3	11.7	599.0	12.4	595	318	0	9.73	2.0	.1026	3.9	10.27	2.0	.0598	14.4	0.80	14.8	.0971	2.1	.139
MJ-649-2.1	0.00147	8	2.59	365	362	1.02	33.4	~~635.1~~	~~11.8~~	636.8	12.4	600	179	-6	9.39	1.9	.0812	4.1	9.64	2.0	.0599	8.1	0.86	8.5	.1035	2.0	.230
MJ-649-3.1	0.00006	65	0.10	340	282	0.86	28.6	600.7	11.1	600.7	11.3	598	26	0	10.23	1.9	.0607	0.8	10.24	1.9	.0599	1.2	0.81	2.3	.0977	1.9	.845
MJ-649-4.1	0.00018	49	0.33	190	105	0.57	17.3	~~650.0~~	~~12.6~~	651.7	12.9	574	55	-12	9.39	2.0	.0619	1.0	9.42	2.0	.0592	2.5	0.87	3.3	.1061	2.0	.628
MJ-649-5.1	0.00009	57	0.15	234	152	0.67	19.9	607.5	11.3	607.7	11.5	600	33	-1	10.10	1.9	.0612	0.9	10.12	1.9	.0599	1.5	0.82	2.5	.0988	1.9	.785
MJ-649-6.1	0.00032	21	0.58	318	251	0.82	26.4	591.5	11.0	590.5	11.2	655	46	11	10.34	1.9	.0661	0.8	10.40	1.9	.0614	2.1	0.81	2.9	.0961	1.9	.675
MJ-649-7.1	0.00007	69	0.13	225	143	0.66	19.0	604.9	11.4	605.0	11.6	602	33	-1	10.15	2.0	.0610	0.9	10.16	2.0	.0599	1.5	0.81	2.5	.0984	2.0	.786
MJ-649-6.2	0.00011	51	0.20	221	89	0.41	18.7	604.1	11.3	604.2	11.5	603	37	0	10.16	1.9	.0616	0.9	10.18	2.0	.0600	1.7	0.81	2.6	.0982	2.0	.754
MJ-649-8.1	0.00003	86	0.06	261	182	0.72	22.1	606.8	11.3	606.6	11.5	618	24	2	10.13	1.9	.0609	0.9	10.13	1.9	.0604	1.1	0.82	2.3	.0987	1.9	.864
MJ-649-9.1	0.00011	25	0.19	403	274	0.70	34.8	615.9	11.4	616.3	11.6	595	22	-3	9.96	1.9	.0613	0.7	9.97	1.9	.0598	1.0	0.83	2.2	.1002	1.9	.886
MJ-649-10.1	0.00008	54	0.15	308	61	0.21	26.1	605.7	11.2	605.8	11.4	602	30	-1	10.14	1.9	.0612	0.8	10.15	1.9	.0600	1.4	0.81	2.4	.0985	1.9	.811
MJ-649-10.2	0.00013	78	0.24	129	109	0.87	10.9	605.2	11.5	604.4	11.7	650	60	7	10.13	2.0	.0632	1.2	10.16	2.0	.0613	2.8	0.83	3.4	.0984	2.0	.581
MJ-649-11.1	0.00011	48	0.19	156	106	0.70	13.3	605.7	11.4	605.8	11.6	603	38	0	10.13	2.0	.0616	1.1	10.15	2.0	.0600	1.7	0.81	2.6	.0985	2.0	.748
MJ-649-12.1	0.00001	179	0.02	218	149	0.71	18.8	615.4	11.4	615.5	11.7	615	22	0	9.98	1.9	.0605	0.9	9.98	1.9	.0603	1.0	0.83	2.2	.1002	1.9	.884
MJ-649-13.1	0.00033	21	0.58	267	132	0.51	22.3	593.0	11.1	593.3	11.3	585	47	-1	10.32	1.9	.0642	0.8	10.38	2.0	.0595	2.2	0.79	2.9	.0963	2.0	.668
MJ-649-14.1	0.00011	45	0.20	174	118	0.70	14.8	606.9	11.4	607.0	11.6	604	37	0	10.11	2.0	.0617	1.1	10.13	2.0	.0600	1.7	0.82	2.6	.0987	2.0	.758
MJ-649-14.2	0.00006	4	0.11	273	84	0.32	23.4	614.2	11.4	614.3	11.6	608	19	-1	9.99	1.9	.0610	0.8	10.00	1.9	.0601	0.9	0.83	2.1	.1000	1.9	.913
MJ-649-15.1	0.00006	68	0.11	330	250	0.78	28.2	609.3	11.3	609.2	11.5	616	28	1	10.08	1.9	.0612	0.8	10.09	1.9	.0603	1.3	0.82	2.3	.0991	1.9	.834
MJ-649-16.1	-0.00002	49	-0.03	230	108	0.48	19.8	616.4	11.5	616.4	11.7	616	20	0	9.97	1.9	.0601	0.9	9.97	1.9	.0603	0.9	0.83	2.2	.1003	1.9	.900
Zircon																											
OM-629-1.1	0.00010	21	0.18	484	300	0.64	40.8	602.0	4.9	602.1	5.0	600	19	0	10.20	0.8	.0614	0.6	10.22	0.8	.0599	0.9	0.81	1.2	.0979	0.8	.703
OM-629-2.1	0.00009	12	0.15	225	123	0.57	19.7	626.4	5.5	626.8	5.6	609	21	-3	9.78	0.9	.0614	0.9	9.80	0.9	.0602	1.0	0.85	1.3	.1020	0.9	.692
OM-629-3.1	0.00010	38	0.18	316	172	0.56	27.0	611.5	5.1	611.3	5.2	625	27	2	10.03	0.9	.0621	0.7	10.05	0.9	.0606	1.2	0.83	1.5	.0995	0.9	.573
OM-629-4.1	0.00013	41	0.23	193	86	0.46	16.6	613.6	5.4	613.9	5.5	603	36	-2	9.99	0.9	.0619	0.9	10.01	0.9	.0600	1.7	0.83	1.9	.0999	0.9	.483
OM-629-5.1	0.00004	34	0.08	285	196	0.71	24.4	611.9	5.1	611.8	5.2	618	19	1	10.04	0.9	.0610	0.8	10.04	0.9	.0604	0.9	0.83	1.2	.0996	0.9	.710
OM-629-6.1	0.00022	45	0.39	64	80	1.30	5.6	622.7	8.2	623.3	8.3	601	66	-4	9.82	1.4	.0631	1.6	9.86	1.4	.0599	3.0	0.84	3.3	.1014	1.4	.412
OM-629-7.2	0.00040	13	0.72	475	219	0.48	42.1	629.1	5.2	629.8	5.3	608	43	-3	9.68	0.9	.0660	0.6	9.75	0.9	.0601	1.9	0.85	2.2	.1025	0.9	.402

Continue...

Appendix 1. Continuation.

Spot Name	204 /206	% err	% comm 206	ppm U	ppm Th	$^{232}Th/^{238}U$	ppm Rad 206Pb	204 corr $^{206}Pb/^{238}U$ Age	1σ err	207 corr $^{206}Pb/^{238}U$ Age	1σ err	204 corr $^{207}Pb/^{206}Pb$ Age	1σ err	% Dis- cor- dant	Total 238 /206	% err	Total 207 /206	% err	238/ 206r	% err	207r /206r	% err	207r /235	% err	206r /238	% err	err correl.
OM-629-8.1	0.00020	45	0.35	64	56	0.89	5.6	619.5	8.7	621.0	8.9	555	62	-10	9.88	1.5	.0615	1.6	9.91	1.5	.0587	2.9	0.82	3.2	.1009	1.5	.458
OM-629-9.1	0.00004	125	0.06	71	63	0.92	19.6	1787.9	16.7	1751.2	19.0	2066	15	16	3.13	1.1	.1282	0.7	3.13	1.1	.1277	0.8	5.63	1.4	.3196	1.1	.791
OM-629-10.1	0.00003	216	0.05	72	78	1.12	6.3	629.0	6.6	628.1	6.7	670	46	7	9.75	1.1	.0623	1.6	9.76	1.1	.0619	2.1	0.87	2.4	.1025	1.1	.456
OM-629-11.1	-0.00009	48	-0.16	144	118	0.85	12.6	623.6	5.7	622.1	5.8	691	33	11	9.86	1.0	.0611	1.1	9.85	1.0	.0625	1.5	0.88	1.8	.1016	1.0	.530
OM-629-12.1	-0.00035	53	-0.62	45	42	0.96	3.9	622.6	8.1	623.3	8.5	578	172	-7	9.93	1.3	.0542	7.0	9.87	1.4	.0593	7.9	~~0.83~~	~~8.0~~	~~.1014~~	~~1.4~~	~~.170~~
OM-629-13.1	0.00006	100	0.10	115	86	0.77	10.1	625.3	8.3	624.7	8.4	655	40	5	9.81	1.4	.0623	1.2	9.82	1.4	.0615	1.9	0.86	2.3	.1019	1.4	.598
OM-629-14.1	0.00050	27	0.88	151	72	0.49	12.8	600.5	5.6	601.5	5.6	565	85	-6	10.15	1.0	.0662	1.1	10.24	1.0	.0590	3.9	0.79	4.0	.0976	1.0	.244
OM-629-15.1	0.00074	18	1.32	112	40	0.37	9.9	624.4	7.7	624.5	7.9	642	95	3	9.70	1.3	.0718	1.5	9.83	1.3	.0611	4.4	0.86	4.6	.1017	1.3	.282
OM-629-16.1	0.00004	62	0.08	372	225	0.62	31.4	605.1	5.0	604.7	5.1	622	22	3	10.15	0.9	.0611	0.8	10.16	0.9	.0605	1.0	0.82	1.4	.0984	0.9	.640
OM-629-17.1	0.00008	43	0.14	398	170	0.44	34.5	617.6	5.1	617.2	5.2	639	23	3	9.93	0.9	.0621	0.6	9.94	0.9	.0610	1.1	0.85	1.4	.1005	0.9	.622
OM-629-18.1	0.00003	91	0.05	151	78	0.53	12.9	610.9	5.6	611.6	5.7	575	29	-6	10.05	1.0	.0596	1.2	10.06	1.0	.0592	1.3	0.81	1.7	.0994	1.0	.582
OM-629-19.1	0.00001	355	0.01	297	203	0.71	25.8	621.8	5.3	621.3	5.4	648	22	4	9.87	0.9	.0614	0.8	9.87	0.9	.0613	1.0	0.86	1.4	.1013	0.9	.652
OM-629-20.1	-0.00003	1	-0.05	103	68	0.69	9.0	625.8	6.1	624.9	6.2	669	29	7	9.81	1.0	.0614	1.3	9.81	1.0	.0619	1.3	0.87	1.7	.1020	1.0	.606
OM-629-20.2	0.00018	15	0.32	181	95	0.54	15.5	608.6	5.4	608.4	5.5	626	29	3	10.07	0.9	.0632	1.0	10.10	0.9	.0606	1.3	0.83	1.6	.0990	0.9	.565
OM-629-21.1	-0.00005	48	-0.10	120	61	0.53	10.2	611.3	5.9	610.5	6.0	648	31	6	10.06	1.0	.0605	1.3	10.05	1.0	.0612	1.4	0.84	1.7	.0995	1.0	.577
OM-629-22.1	0.00001	73	0.01	216	109	0.52	75.5	2200.0	16.3	2200.1	19.6	2200	6	0	2.46	0.9	.1379	0.3	2.46	0.9	.1378	0.3	7.73	0.9	.4067	0.9	.936
OM-629-22.2	0.00003	80	0.05	362	50	0.14	33.9	665.7	5.6	666.5	5.7	631	20	-5	9.19	0.9	.0612	0.7	9.19	0.9	.0608	0.9	0.91	1.3	.1088	0.9	.696
Titanite																											
MJ-649-1.1	0.002200	27	3.85	172	20	0.12	15	599.6	32	601	32	584	408	-3	9.84	5.5	0.091	5.1	10.24	5.6	0.06	19	0.8	20	0.098	5.6	0.3
MJ-649-2.1	0.005200	14	9.27	60	134	2.3	5.3	571.5	30	574	31	578	685	1	9.74	5.2	0.135	6	10.73	5.4	0.06	31	0.76	32	0.093	5.4	0.2
MJ-649-3.1	0.005400	13	9.59	67	142	2.2	6.5	627.3	31	629	33	703	704	12	8.79	5	0.141	8.2	9.73	5.2	0.06	32	0.89	34	0.102	5.2	0.2
MJ-649-4.1	0.002500	11	4.51	249	36	0.15	20.5	561.9	24	563	24	567	270	1	10.46	4.3	0.096	2.5	10.95	4.4	0.06	12	0.74	13	0.091	4.4	0.3
MJ-649-5.1	0.004700	13	8.4	84	220	2.71	7.6	590.1	29	593	30	586	661	-1	9.51	4.9	0.128	8	10.38	5.1	0.06	30	0.79	31	0.096	5.1	0.2
MJ-649-6.1	0.004700	18	8.23	59	129	2.28	5.8	641	35	644	35	662	617	3	8.73	5.4	0.129	4.3	9.52	5.7	0.06	28	0.89	29	0.105	5.7	0.2
MJ-649-7.1	0.005400	15	9.55	54	209	3.98	5.5	653.1	35	656	37	690	713	6	8.43	5.4	0.141	7.1	9.32	5.7	0.06	33	0.92	34	0.107	5.7	0.2
MJ-649-8.1	0.004200	14	7.48	76	169	2.29	6.4	557.2	27	559	27	563	514	1	10.21	4.8	0.12	4.1	11.03	4.9	0.06	23	0.73	24	0.09	5	0.2
MJ-649-9.1	0.002200	14	3.96	120	9	0.08	10.6	602.4	32	603	33	651	255	8	9.78	5.5	0.094	3	10.19	5.6	0.06	12	0.83	13	0.098	5.6	0.4
MJ-649-10.1	0.004200	13	7.46	81	141	1.8	6.8	556.7	27	560	28	519	526	-7	10.22	4.9	0.119	4.3	11.04	5	0.06	24	0.72	25	0.09	5.1	0.2
MJ-649-11.1	0.002659	11	4.72	119	276	2.39	10.6	602.0	36.5	602.9	37.2	636	263	6	9.71	6.3	.0994	1.1	10.19	6.3	.0609	11.9	0.82	13.8	.0979	6.3	.461
MJ-649-12.1	0.003547	11	6.31	120	401	3.46	10.4	580.7	35.7	576.8	36.2	862	301	48	9.91	6.4	.1188	1.2	10.57	6.4	.0678	14.1	0.88	15.8	.0943	6.4	.405
MJ-649-13.1	0.001632	12	2.91	240	244	1.05	19.3	561.7	37.2	562.4	37.9	565	182	1	10.65	6.9	.0827	2.2	10.97	6.9	.0590	8.2	0.74	10.9	.0910	6.9	.637
MJ-649-14.1	0.003728	11	6.61	95	332	3.60	8.8	615.7	38.3	615.4	39.0	739	344	20	9.28	6.4	.1177	1.5	9.94	6.5	.0639	15.9	0.88	17.5	.1002	6.5	.371
MJ-649-15.1	0.003175	13	5.64	89	306	3.54	7.8	591.5	36.6	592.7	37.3	621	332	5	9.79	6.4	.1065	1.4	10.37	6.5	.0605	15.0	0.80	16.7	.0961	6.5	.387
MJ-649-16.1	0.003861	10	6.87	131	463	3.64	11.3	573.3	35.5	575.3	36.2	579	389	1	9.97	6.4	.1154	1.2	10.71	6.5	.0594	17.5	0.76	19.1	.0930	6.5	.339
MJ-649-17.1	0.003232	10	5.75	152	342	2.32	12.9	571.3	34.7	573.3	35.4	555	322	-3	10.14	6.3	.1057	1.1	10.76	6.3	.0587	14.4	0.75	16.1	.0927	6.3	.394
MJ-649-18.1	0.003293	11	5.83	170	613	3.73	15.8	623.1	37.9	625.6	38.7	605	327	-3	9.25	6.3	.1078	1.2	9.82	6.4	.0601	14.7	0.84	16.4	.1015	6.4	.388
MJ-649-19.1	0.000795	12	1.41	579	33	0.06	52.1	633.2	37.4	633.9	38.2	625	78	-1	9.54	6.2	.0721	0.8	9.68	6.2	.0606	3.6	0.86	7.2	.1032	6.2	.862
MJ-649-21.1	0.002214	11	3.92	202	580	2.97	18.2	618.1	37.2	618.9	37.9	645	214	4	9.53	6.3	.0932	1.1	9.91	6.3	.0612	9.7	0.85	11.8	.1006	6.3	.534
Mean			6.11	146.0	240.0	2.2	12.86																				
StD			2.29	117.3	176.3	1.3	10.38																				

Continue...

Appendix 1. Continuation.

Spot Name	204 /206	% err	% comm 206	ppm U	ppm Th	$^{232}Th/^{238}U$	ppm Rad 206Pb	204 corr $^{206}Pb/^{238}U$ Age	1σ err	207 corr $^{206}Pb/^{238}U$ Age	1σ err	204 corr $^{207}Pb/^{206}Pb$ Age	1σ err	% Dis- cor- dant	Total 238 /206	% err	Total 207 /206	% err	238/ 206r	% err	207r /206r	% err	207r /235	% err	206r /238	% err	err correl.
Titanita																											
OM-629-1.1	0.00517	10	9.20	23	146	6.43	4.1	584.3	25.7	587.4	26.3	582	526	0	9.52	4.4	.1345	1.1	10.48	4.6	.0594	23.6	0.78	24.7	.0949	4.6	.186
OM-629-2.1	0.00479	17	8.47	27	168	6.42	2.6	636.5	19.8	639.4	18.9	655	586	3	8.77	2.8	.1308	1.8	9.58	3.2	.0615	26.7	0.88	27.5	.1038	3.3	.120
OM-629-3.1	0.00754	14	13.37	28	188	6.99	2.8	620.6	43.5	624.8	43.5	668	891	8	8.50	6.9	.1710	1.5	9.81	7.3	.0619	40.5	0.86	42.2	.1011	7.3	.174
OM-629-3.2	0.00710	10	12.56	15	100	6.67	3.1	640.2	22.7	647.6	25.3	531	897	-17	8.31	3.3	.1614	6.7	9.50	3.7	.0581	39.8	0.84	41.1	.1044	3.7	.091
OM-629-4.2	0.00094	8	1.67	485	350	0.72	88.4	638.8	13.5	639.5	13.9	634	81	-1	9.43	2.2	.0745	0.5	9.59	2.2	.0609	3.7	0.87	4.4	.1042	2.2	.509
OM-629-5.1	0.00633	12	11.21	37	271	7.62	3.7	630.2	40.3	638.6	41.2	425	797	-33	8.58	6.5	.1477	2.6	9.67	6.7	.0554	34.7	0.78	36.4	.1027	6.7	.184
OM-629-5.2	0.00488	12	8.64	20	151	7.60	3.8	624.9	18.9	626.9	19.2	684	486	9	8.93	2.9	.1329	1.1	9.77	3.1	.0623	22.1	0.87	23.0	.1018	3.2	.138
OM-629-6.2	0.00585	10	10.37	22	136	6.22	4.2	609.1	19.0	612.6	19.7	618	589	1	8.99	3.0	.1452	1.2	10.03	3.3	.0604	26.5	0.83	27.5	.0991	3.3	.119
OM-629-7.2	0.00489	10	8.67	38	209	5.58	7.1	617.2	17.5	620.3	18.1	619	478	0	9.04	2.8	.1314	1.1	9.90	3.0	.0605	21.5	0.84	22.3	.1005	3.0	.133
OM-629-8.2	0.00441	10	7.82	43	274	6.41	8.0	616.7	16.6	620.6	17.2	557	443	-10	9.14	2.7	.1229	1.0	9.92	2.8	.0588	19.7	0.81	20.5	.1004	2.8	.138
OM-629-9.2	0.00703	10	12.45	13	93	6.95	2.7	621.8	20.7	628.2	21.3	545	766	-12	8.58	3.0	.1606	1.2	9.80	3.5	.0585	33.9	0.82	35.2	.1013	3.5	.100
OM-629-10.2	0.00578	7	10.24	74	216	2.90	14.7	629.5	16.8	633.6	18.1	623	529	-1	8.69	2.6	.1444	0.8	9.69	2.8	.0606	23.6	0.86	24.7	.1026	2.8	.113
OM-629-11.1	0.00711	9	12.57	22	162	7.46	2.3	640.7	45.0	648.6	46.5	508	793	-21	8.30	7.2	.1609	2.8	9.49	7.3	.0575	34.9	0.83	36.8	.1045	7.3	.200
OM-629-11.2	0.00640	10	11.35	18	118	6.58	3.5	616.8	19.5	624.3	20.1	447	730	-28	8.77	2.9	.1493	1.2	9.89	3.3	.0559	31.8	0.77	33.0	.1004	3.3	.101
OM-629-12.2	0.00205	9	3.63	213	487	2.28	39.7	639.6	14.2	642.0	14.6	590	188	-8	9.22	2.3	.0894	0.6	9.57	2.3	.0596	8.4	0.86	9.0	.1043	2.3	.261
OM-629-15.2	0.00142	7	2.52	232	260	1.12	82.6	618.9	11.5	620.5	11.8	582	123	-6	9.66	1.9	.0800	0.5	9.91	1.9	.0594	5.5	0.83	6.0	.1008	1.9	.325
OM-629-16.1	0.00334	8	5.92	60	298	5.10	5.5	615.8	41.4	616.1	42.3	699	284	13	9.35	7.0	.1110	0.9	9.94	7.0	.0627	13.0	0.87	15.1	.1002	7.0	.466
OM-629-16.2	0.00394	9	6.99	56	283	5.10	20.7	617.5	14.1	619.5	14.6	639	365	4	9.21	2.2	.1181	0.9	9.91	2.4	.0610	16.5	0.85	17.2	.1005	2.4	.139
OM-629-17.1	0.00647	10	11.44	20	122	6.44	2.0	649.6	44.8	654.3	46.0	654	666	1	8.29	7.0	.1552	2.6	9.36	7.2	.0615	30.1	0.90	31.9	.1060	7.2	.226
OM-629-17.2	0.00179	9	3.17	160	294	1.84	57.2	618.9	12.0	619.6	12.3	638	158	3	9.59	2.0	.0869	0.9	9.91	2.0	.0610	7.2	0.85	7.6	.1008	2.0	.266
OM-629-18.1	0.00456	9	8.09	35	185	5.44	3.2	600.5	40.4	600.7	41.2	726	407	21	9.37	7.0	.1294	1.1	10.19	7.0	.0635	18.6	0.86	20.4	.0976	7.0	.344
OM-629-18.2	0.00185	8	3.28	154	289	1.87	55.3	620.0	12.0	619.8	12.3	682	157	10	9.56	2.0	.0890	0.6	9.89	2.0	.0622	7.1	0.87	7.6	.1010	2.0	.265
OM-629-19.1	0.00703	10	12.51	18	154	8.62	1.7	581.5	40.8	587.6	41.8	479	790	-18	9.20	7.1	.1592	1.3	10.52	7.3	.0567	34.6	0.74	36.5	.0944	7.3	.200
OM-629-19.2	0.00313	9	5.56	39	106	2.72	14.2	612.8	13.1	620.1	13.5	320	351	-48	9.44	2.2	.0987	0.9	10.00	2.2	.0528	15.0	0.73	15.6	.0997	2.2	.144
OM-629-20.1	0.00535	7	9.49	148	249	1.69	28.5	620.7	17.4	621.0	18.6	766	444	23	8.90	2.8	.1420	0.8	9.84	2.9	.0648	20.4	0.90	21.3	.1011	2.9	.138
OM-629-20.2	0.00630	7	11.18	61	86	1.46	5.9	605.6	13.8	609.2	15.4	627	584	3	8.96	2.1	.1520	1.1	10.08	2.4	.0607	26.2	0.82	27.2	.0985	2.4	.088
OM-629-21.1	0.00618	11	10.97	10	84	8.02	4.0	605.3	22.2	612.6	22.6	422	762	-30	8.98	3.5	.1455	2.6	10.09	3.8	.0553	33.2	0.75	34.4	.0984	3.9	.112
OM-629-22.1	0.00587	10	10.43	18	149	8.40	6.6	594.9	15.8	601.2	16.4	448	651	-25	9.21	2.4	.1416	1.1	10.28	2.8	.0559	28.4	0.74	29.4	.0967	2.8	.095
OM-629-23.1	0.00393	10	6.97	48	260	5.48	17.9	621.4	14.3	625.1	14.7	562	388	-10	9.16	2.3	.1160	1.0	9.84	2.4	.0589	17.3	0.82	18.0	.1012	2.4	.134
OM-629-24.1	0.00513	9	9.10	34	169	5.04	12.6	610.2	15.0	613.2	15.8	622	500	2	9.11	2.3	.1350	1.6	10.02	2.6	.0605	22.5	0.83	23.3	.0993	2.6	.111
OM-629-25.1	0.00356	9	6.31	66	241	3.67	24.5	622.4	14.0	625.4	14.5	588	337	-6	9.21	2.2	.1113	0.9	9.83	2.3	.0596	15.1	0.83	15.7	.1014	2.4	.150
OM-629-26.1	0.00300	9	5.31	61	204	3.32	22.2	610.5	13.4	612.9	13.8	578	282	-5	9.50	2.2	.1028	0.8	10.04	2.3	.0593	12.6	0.81	13.2	.0993	2.3	.174
OM-629-27.1	0.00476	10	8.47	29	159	5.45	10.5	588.8	14.6	591.9	15.2	569	478	-3	9.52	2.4	.1283	1.0	10.41	2.6	.0591	21.4	0.78	22.1	.0956	2.6	.118
OM-629-28.1	0.00453	9	8.04	43	187	4.39	15.3	589.6	13.9	594.3	14.5	476	470	-19	9.56	2.3	.1226	1.0	10.39	2.5	.0566	20.6	0.75	21.4	.0958	2.5	.116
OM-629-29.1	0.00333	10	5.88	59	214	3.62	22.7	641.8	14.7	645.6	15.2	567	323	-12	8.96	2.3	.1073	0.9	9.52	2.4	.0590	14.4	0.85	15.0	.1047	2.4	.160
OM-629-34.1	0.00152	8	2.70	118	152	1.29	101.3	628.9	11.8	631.8	12.1	536	140	-15	9.48	1.9	.0803	0.6	9.74	2.0	.0582	6.2	0.82	6.7	.1025	2.0	.294
OM-629-30.1	0.00415	10	7.36	48	240	4.97	17.9	610.7	14.3	612.9	14.8	630	396	3	9.28	2.3	.1209	1.0	10.02	2.4	.0608	17.9	0.83	18.6	.0994	2.5	.132
OM-629-31.1	0.00351	7	6.22	196	256	1.31	71.2	608.2	15.6	608.6	16.3	695	291	14	9.44	2.6	.1133	0.7	10.07	2.7	.0626	13.2	0.85	13.9	.0989	2.7	.193
OM-629-32.1	0.00251	8	4.45	209	394	1.89	75.4	616.5	12.2	617.3	12.6	648	217	5	9.50	2.0	.0976	0.7	9.94	2.1	.0613	9.8	0.85	10.3	.1004	2.1	.201
OM-629-33.1	0.00535	7	9.49	109	211	1.93	40.8	601.9	13.5	605.9	14.7	566	500	-6	9.20	2.1	.1367	0.8	10.16	2.3	.0590	22.2	0.80	23.1	.0979	2.4	.102
Mean			8.1	77.7	207.8	4.7	22.8																				
StD			3.2	90.7	86.6	2.4	27.4																				

Strikethrough values correspond to excluded data.
Comm: common Pb; err: error; Rad: radiogenic (r); corr: corrected; correl.: correlation.